Available online at www.sciencedirect.com
SCIENCE DIRECT
Polymer 46 (2005) 10970–10981
polymer
www.elsevier.com/locate/polymer

Theoretical studies on the electronic and optical properties of two thiophene–fluorene based π-conjugated copolymers

Li Yang[a], Ji-Kang Feng[a,b,*], Ai-Min Ren[a]

[a] State Key Laboratory of Theoretical and Computational Chemistry, Institute of Theoretical Chemistry, Jilin University, Changchun 130023, China
[b] College of Chemistry, Jilin University, Changchun 130023, China

Received 15 July 2005; received in revised form 13 September 2005; accepted 13 September 2005
Available online 29 September 2005

Abstract

The low PL quantum efficiency, typically 1–3%, in solid film, limits the application of polythiophene and derivatives (PTs) in PLEDs. The six-member aromatic rings polyfluorenes (PFs) with higher PL efficiencies have been introduced into the backbone of PTs, in an effort to develop highly efficient, desirable charge carrier transporting and low energy gap thiophene–fluorene based light-emitting polymers. In this contribution, quantum-chemical techniques are employed to study two fluorene–thiophene incorporated π-conjugated polymers, namely, poly((5,5-*E*-α-(2-thienyl)methylene)-2-thiopheneacetonitrile)-*alt*-2,7-(9,9-dimethylfluorene) (PFTCNVT) and poly((5,5″-(3′,4′-dimethyl-2,2′;5′,2″-terthiophene1′,1′-dioxide))-*alt*-2,7-(9,9-dimethylfluorene)) (PFTORT). Density functional theory (DFT) and time-dependent DFT approaches are employed to study the neutral molecules, positive and negative ions, the IPs and EAs, HOMO–LUMO gaps (Δ_{H-L}), as well as the lowest excitation energies (E_gs). It is interesting to note that the two copolymers PFTCNVT and PFTORT are superior to the properties of pristine polyfluorene (PF) and polythiophene (PT). In addition to the improved PL efficiency, they still presented lower energy-gap comparable to PTs. Furthermore, the LUMO energies lower about 1.4 eV and thus the EAs increase around 1.4 eV in PFTCNVT and PFTORT compared with PFs, suggesting the significant improved electron-accepting and transporting abilities in the two copolymers. These properties can be explained by the presence of more electron-accepting thiophene units in the repeated unit of the copolymers and the more planar conformations in the two copolymers under study.

Keywords: Fluorene; Thiophene; DFT

1. Introduction

Following the discovery of electroluminescene (EL) in a conjugated polymer, enormous efforts have been made toward the development of conjugated polymers as light-emitting materials [1–9]. In the categories of conjugated polymers, polythiophene and derivatives (PTs) have attracted considerable attention due to their attractive characters of good stability both in neutral state and in doped states and their wide electronic and optical tunability [10–12]. By attaching different functional groups and controlling regioregularity and steric interaction, light emission ranging from blue to near-infrared spectra has been demonstrated in PTs [13,14]. Unfortunately, PTs exhibit very low photoluminescence (PL) quantum efficiency, which is one of the most considerations in developing conjugated polymers for PLEDs [15,16]. In fact, most of other conjugated polymers, especially those based on six-member aromatic rings, such as poly(*p*-phenylenevinylene) and derivatives (PPVs) [17], substituted poly(*p*-phenylenes) (PPPs) [18] and stustituted polyfluorenes (PFs) [19–24] generally have much higher PL efficiencies than PTs. Especially the PFs have emerged as the most promising light-emitting materials due to their emission at wavelength spanning the entire visible spectrum, high fluorescence efficiency, and good thermal stability. In addition to excellent luminescent properties, OLEDs also need adequate and balanced transport of both injected electrons and holes to allow an efficient recombination of these electrical charges in the luminescent chromophore [25–28]. Many ways have been used to modulate the ionization potential (IP), electron affinity (EA), and band gap including conjugation length control, as well as the introduction of electron-donating or -accepting groups on the conjugated polymer's backbone, which produces

* Corresponding author. Address: State Key Laboratory of Theoretical and Computational Chemistry, Institute of Theoretical Chemistry, Jilin University, Changchun 130023, China. Tel.: +86 431 8499592; fax: +86 431 8945942.
E-mail address: jikangf@yahoo.com (J.-K. Feng).

0032-3861/$ - see front matter © 2005 Elsevier Ltd. All rights reserved.
doi:10.1016/j.polymer.2005.09.050

a remarkable influence on its electrical, electrochemical and optical properties.

In order to rationalize the experimentally observed properties of known materials [29–36] and to predict those of unknown ones [37–39], theoretical investigations on the structures and electronic spectra and emissive properties of these materials are indispensable. In the past decades, ab initio and semiempirical levels were applied to analyze various properties of oligomers and polymers. Schulten et al. present a multireference double excitation configuration interaction method (MRD-CI) and employ a Pariser–Parr–Pople (PPP) model Hamiltonian in polyenes [40]. Brédas used HF semiempirical AM1 and INDO Hamiltonians to predict nonlinear optical response and simulate the frequency-dependent response in poly(*p*-phenylenevinylene) [41]. On the other hand, correlation effects can be very important for the study of electronic structure of molecules and should be taken into account particularly when one is interested in the evaluation of the energy gap. In this sense, density functional theory (DFT), due to its feature of including the electronic correlation in a computationally efficient manner, can be used in larger molecular systems. So, recently, a series of polymers were studied employing DFT and TDDFT methods by McKee [42], Yu [43], Jiang et al. [44]. However, with the growing molecular size from monomer to oligomers, it is very difficult to use a high level of theory to treat these systems.

In this paper, we insert a fluorene ring into the backbone of two thienyl-based units, 5,5-*E*-α-(2-thienyl)methylene)-2-thiopheneacetonitrile (TCNVT) and 5,5″-3′,4′-dimethyl-2,2′;5′,2″-terthiophene1′,1′-dioxide (TORT), in an effort to develop highly efficient thiophene–fluorene-based light-emitting copolymers (as depicted in Fig. 1), in which the solid-state PL quantum yields has been improved [45]. For better understanding of the electronic properties of oligomers and polymers, theoretical studies usually place emphasis on their ground-state geometries, band gaps and low-lying excited states by density functional theory (DFT), time-dependent DFT (TDDFT), and singlet configuration interaction (CIS) methods. Then we apply the experimentally well-known reciprocal rule for polymers, which states that many properties of homopolymers tend to vary linearly as functions of reciprocal chain lengths [44,46–53]. A distinct advantage of this approach is that it can provide the convergence behavior of the structural and electronic properties of oligomers. Whether and how this incorporation between the fluorene and thiophene-based groups would modulate the optical and electronic characters will be demonstrated in this work, through exploring and comparing the energies of HOMO and LUMO and the variation of IPs and EAs and especially the energy gap of polymers PFTCNVT and PFTORT with pristine PF and PT. On the other hand, we wanted to show the potential of a quantum mechanical modeling based on DFT, in the evaluation of ground and excited state properties of oligomers and polymers by comparison with the available experimental data.

2. Computational details

All calculations on these oligomers studied in this work have been performed on the SGI origin 2000 server using Gaussian 03 program package [54]. Calculations on the electronic ground state were carried out using density functional theory (DFT), B3LYP/6-31G*. The investigated polymers $(FTCNVT)_n$ and $(FTORT)_n$ correspond to copolymers in literature 45, PFTCNVT and PFTORT, respectively, and the main difference is that the hexyl groups at 3′,4′-positions in terthiophene-1,1-dioxide and that groups at 9-position in fluorene ring have been replaced by methyl, respectively, for the sake of reducing the time of calculation. It has been proved that the presence of alkyl groups does not significantly affect the equilibrium geometry and thus the electronic and the optical properties [55,56]. In the subsequent parts, the calculated values are all compared with the experimental data for corresponding copolymers in Ref. [45]. To determine the minimum energy configuration as well as energy differences between the syn- and anti-conformation, we perform full geometry optimization on the monomer of $(FTCNVT)_n$ with B3LYP/6-31G*. Density functional single-point calculations have been performed using the 6-31+G* and 6-31+G** basis sets, respectively. The results show that the anti-conformation is only slightly more stable than the

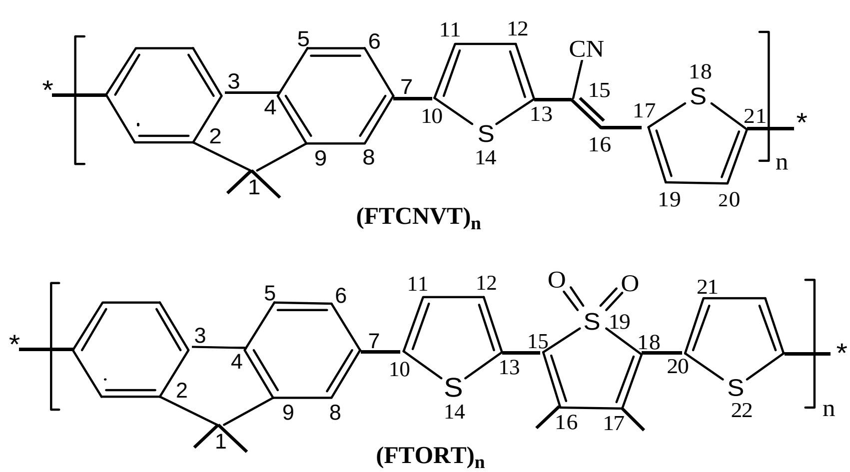

Fig. 1. The sketch map of the structures.

Table 1
Selected inter-ring dihedral angles and bond lengths of $(FTCNVT)_n$ and $(FTORT)_n$ ($n=1$–4) in the ground obtained by B3LYP/6-31G* calculations

	$(FTCNVT)_n$				$(FTORT)_n$			
(n)	(1)	(2)	(3)	(4)	(1)	(2)	(3)	(4)
Dihedral angles								
Φ(2,3,4,9)	0.1	0.2	0.0	0.1	0.1	0.2	0.1	0.0
Φ(8,7,10,14)	25.5	25.4	24.6	24.5	25.1	25.9	25.8	23.6
Φ(14,13,15,16)	1.6	0.6	2.2	2.6	26.3	28.1	27.4	25.6
Φ(15,16,17,18)	0.1	1.4	0.9	1.4				
Φ(19,18,20,21)					31.5	27.0	29.1	30.5
Bond lengths								
r(3,4)	1.466	1.466	1.466	1.466	1.466	1.466	1.466	1.466
r(7,10)	1.464	1.463	1.463	1.463	1.464	1.464	1.464	1.464
r(13,15)	1.459	1.458	1.458	1.458	1.440	1.441	1.441	1.440
r(15,16)	1.369	1.371	1.371	1.371				
r(16,17)	1.435	1.431	1.431	1.431				
r(18,20)					1.445	1.441	1.441	1.441

syn- one by 0.07 and 0.11 kcal mol^{-1} based on 6-31+G* and 6-31+G** basis sets, respectively. And both structures have similar bond lengths, angles and nearly equal HOMO–LUMO gap, suggesting the gauche conformation has slight effects on the structure, and thus the electronic and optical properties. The selected important inter-ring bond lengths and dihedral angles of $(FTCNVT)_n$ and $(FTORT)_n$ ($n=1$–4) in the neutral ground state obtained by B3LYP/6-31G* calculations are listed in Table 1. The results of the optimized structures for the two series of copolymeric molecules show that the bond lengths and bond angles do not vary significantly with the oligomer size in the series of $(FTCNVT)_n$, as well as $(FTORT)_n$. And it suggests that we can describe the basic structures of the polymers as their oligomers. As already mentioned before, one of the most important features of the π-conjugated polymers is their ability to become highly conducting after oxidative (p-type) or reductive (n-type) doping. So, the cationic and anionic geometries of oligomers in both series of $(FTCNVT)_n$ and $(FTORT)_n$ ($n=1$–4) are optimized by B3LYP/6-31G* and the inter-ring torsional angles as well as bond lengths between two adjacent units are compiled in Table 2. The optimized geometries of the ions were then used to calculate the ionization potential and electron affinity energies.

There are two theoretical approaches for evaluating the energy gap in this paper. One way is based on the ground-state properties, from which the band gap is estimated from the energy difference between the highest occupied molecular orbital (HOMO) and the lowest unoccupied molecular orbital (LUMO) [57–59], when $n=\infty$, termed the HOMO–LUMO gaps (Δ_{H-L}s). The TDDFT, which has been used to study

Table 2
Selected dihedral angles and inter-ring bond lengths of $(FTCNVT)_n$ and $(FTORT)_n$ ($n=1$–4) in the cationic and anionic states obtained by DFT//B3LYP/6-31G* calculations

(n)	(1)	(2)	(3)	(4)	(1)	(2)	(3)	(4)
	Cationic state				Anionic state			
$(FTCNVT)_n$								
Φ(2,3,4,9)	0.0	0.0	0.1	0.2	0.0	0.0	0.1	0.1
Φ(8,7,10,14)	0.0	0.0	3.7	5.4	0.0	0.0	3.7	0.9
Φ(14,13,15,16)	0.0	0.0	0.4	0.0	0.0	0.1	0.7	0.4
Φ(15,16,17,18)	0.0	0.0	0.0	0.2	0.0	0.0	0.2	0.1
r(3,4)	1.447	1.458	1.462	1.464	1.460	1.466	1.459	1.459
r(7,10)	1.428	1.442	1.449	1.451	1.436	1.451	1.450	1.453
r(13,15)	1.428	1.432	1.440	1.444	1.430	1.443	1.446	1.448
r(15,16)	1.396	1.393	1.386	1.383	1.413	1.398	1.387	1.386
r(16,17)	1.408	1.408	1.415	1.418	1.407	1.406	1.416	1.417
$(FTORT)_n$								
Φ(2,3,4,9)	0.0	0.0	0.0	0.1	0.0	0.1	0.1	0.1
Φ(8,7,10,14)	0.4	1.1	8.4	8.5	0.2	9.7	8.2	12.2
Φ(14,13,15,16)	7.1	9.1	14.4	17.9	9.1	7.1	16.5	23.7
Φ(19,18,20,21)	16.6	17.6	19.8	22.2	24.8	24.7	20.9	20.2
r(3,4)	1.449	1.454	1.453	1.456	1.462	1.460	1.472	1.460
r(7,10)	1.429	1.443	1.448	1.450	1.441	1.446	1.452	1.454
r(13,15)	1.394	1.401	1.411	1.410	1.400	1.408	1.415	1.417
r(18,20)	1.406	1.405	1.413	1.418	1.416	1.424	1.425	1.419

systems of increasing complexity due to its relatively low computational cost and also to include in its formalism the electron correlation effects, is also employed to extrapolate energy gap of polymers from the calculated first dipole-allowed excitation energy of their oligomers. The excited geometries have been optimized by ab initio CIS/3-21G* [60]. Based on the excited geometries, the emission spectra of part of the molecules are investigated. We employed the linear extrapolation technique in this research [44], which has been successfully employed to investigate several series of polymers [31,42,44,46,61]. The linearity between the calculated IPs, EAs, $\Delta_{\mathrm{H-L}}$s and E_{g}s of the oligomers and the reciprocal chain length is excellent for both homologous series of oligomers.

3. Results and discussion

3.1. Ground states structural properties

In fact, because the dihedral angle between two phenyl rings in fluorene segment of the series of oligomers is fixed by ring bridged-atoms which tend to keep the fluorene ring quasi planar conformation, the dihedral angles in fluorene are no more than 1°. As shown in Table 1, the biggest dihedral angle in $(\mathrm{FTCNVT})_n$ is $\Phi(8,7,10,14)$, which averages around 25° in the oligomers in the neutral state. And in $(\mathrm{FTORT})_n$ there are three significant twists, $\Phi(8,7,10,14)$, $\Phi(14,13,15,16)$ and $\Phi(19,18,20,21)$ with average values around 25, 26 and 30°, respectively. That is the segments in bridge-bond between adjacent fluorene and thienyl rings or the two adjacent thienyl rings are twisted. Importantly, the larger dihedral angle between the two joint fluorenes is observed in $(\mathrm{F})_n$ (average value is 37°) [46] than that in $(\mathrm{FTCNVT})_n$ and $(\mathrm{FTORT})_n$, indicating the nicer π conjugated structures are obtained in the latter two due to the cooperation with two thienyl-based electron-accepting moieties. Furthermore, the planar characteristic of vinyl group in $(\mathrm{FTCNVT})_n$ farther boosts the whole conjugation for the conjugated backbones as depicted in Fig. 2.

3.2. Frontier molecular orbitals

It will be useful to examine the highest occupied orbitals and the lowest virtual orbitals for these oligomers because the relative ordering of the occupied and virtual orbitals provides a reasonable qualitative indication of the excitation properties and of the ability of electron or hole transport. In general, as plotted in Fig. 3 the HOMO possesses an antibonding character between the consecutive subunits. This may explain the non-planarity observed for these oligomers in their ground states. On the other hand, the LUMO of all the oligomers generally shows a bonding character between the subunits. This implies that the singlet-excited state involving mainly the promotion of an electron from the HOMO to the LUMO should be more planar. For LUMO in both $(\mathrm{FTCNVT})_n$ and $(\mathrm{FTORT})_n$, the electronic clouds transfer to the right parts from fluorene rings and strongly confined to TCNVT and FTORT moieties due to electronegative sulphur heteroatoms and especially in PFTORT, the LUMOs are predominantly on 3′,4′-dimethyl-2,2′;5′,2″-terthiophene1′,1′-dioxide by the presence of the oxygen atoms. For the polymers, this implies the TCNVT and FTORT serve as electron-accepting moieties for electronic materials and is anticipated to have improved electron affinities owing to the strong electron-accepting thiophene-based groups on the polymer backbone.

In experiment, the HOMO and LUMO energies were calculated from one empirical formula proposed by Brédas et al., based on the onset of the oxidation and reduction peaks measured by cyclic voltammetry, assuming the absolute energy level of ferrocene/ferrocenium to be 4.8 eV below vacuum [31]. Whereas the HOMO and LUMO energies can be calculated by density functional theory (DFT) in this study. However, it is noticeable that solid-state packing effects do not included in the DFT calculations, which tends to significantly reduce the torsion angles between adjacent units and consequently affects the HOMO and LUMO energy levels in a thin film compared to an isolated molecule as considered in the calculations. Even if these calculated HOMO and LUMO energy levels are not accurate, it is possible to use them to get information by comparing similar oligomers and polymers.

Fig. 4 describes the evolution of the B3LYP/6-31G* calculated highest occupied molecular orbital (HOMO) and lowest unoccupied molecular orbital (LUMO) energies as a function of the inverse number of monomer units in $(\mathrm{FTCNVT})_n$ and $(\mathrm{FTORT})_n$. For the sake of comparison, the frontier energy levels of $(\mathrm{F})_n$ ($n=1$–4) are also listed in Fig. 4. As is usual in π-conjugated systems, the energy of the frontier electronic levels evolves linearly with inverse chain length in the four systems: the HOMO energies increase, whereas the LUMO energies decrease [62]. Similar energies are obtained

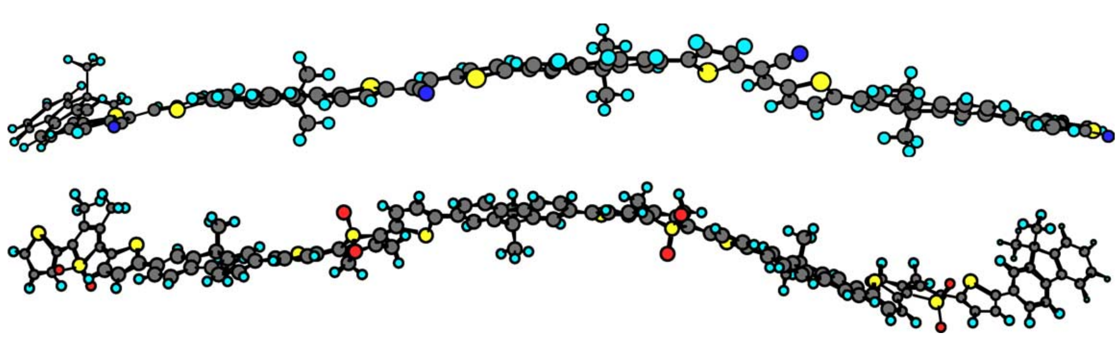

Fig. 2. Optimized structures of $(\mathrm{FTCNVT})_4$ (up) and $(\mathrm{FTORT})_4$ (down).

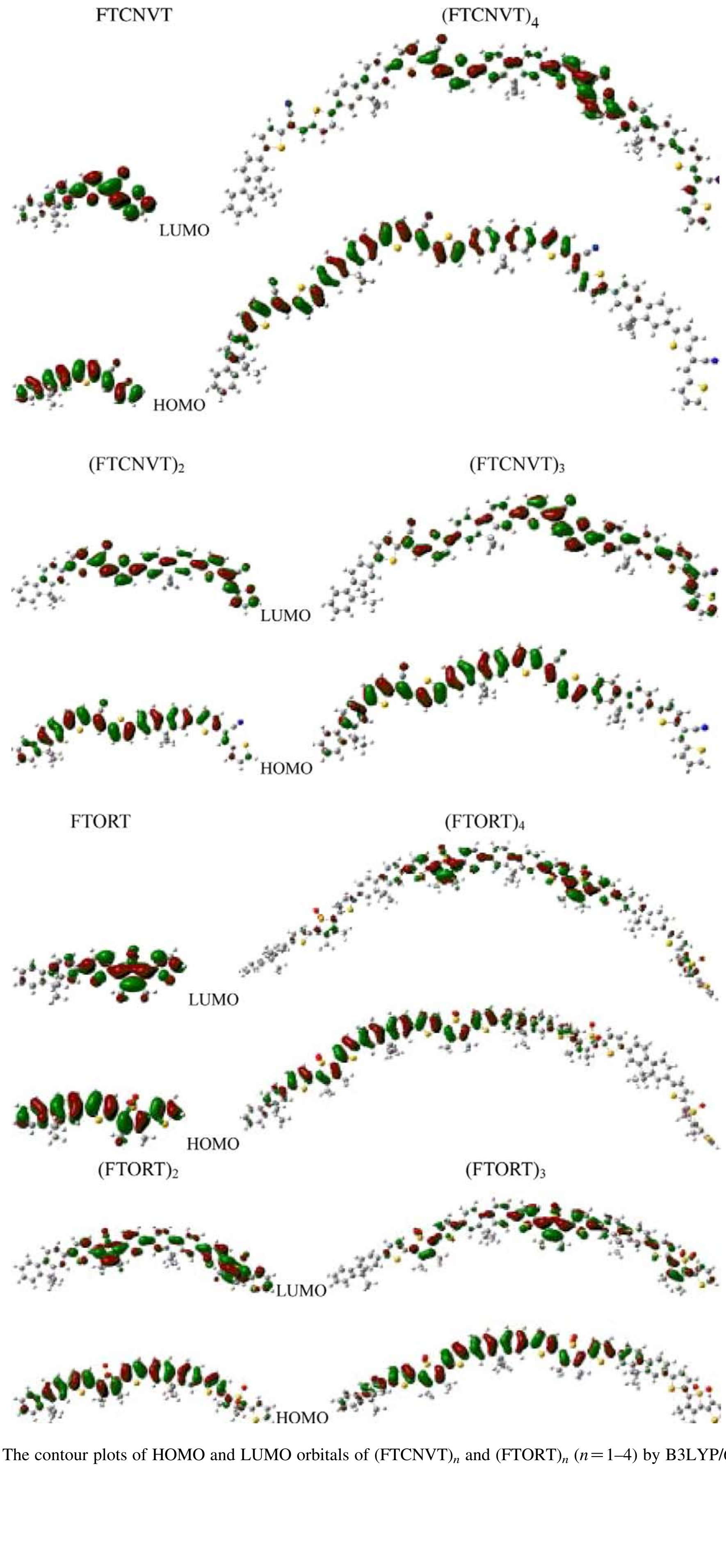

Fig. 3. The contour plots of HOMO and LUMO orbitals of $(FTCNVT)_n$ and $(FTORT)_n$ ($n = 1$–4) by B3LYP/6-31G*.

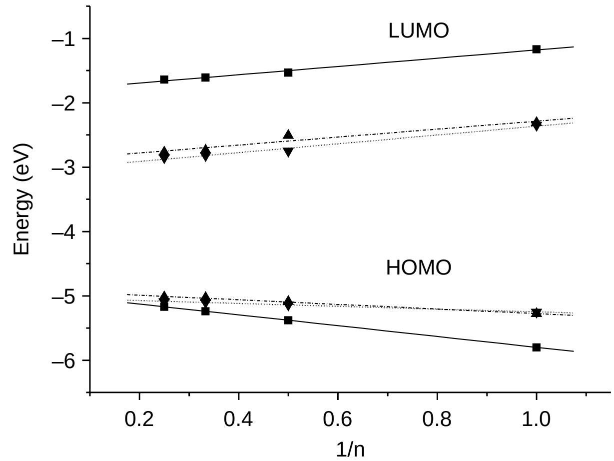

Fig. 4. B3LYP/6-31G* calculated HOMO and LUMO energies of PFTCNVT (dashed dot lines), PFTORT (short dot lines) and PF (solid lines) oligomers as a function of the inverse number of monomer units.

for the HOMO of the longest oligomer of PFTCNVT (∼ −5.1 eV) and PF (∼ −5.2 eV) [46], as well as PFTORT (∼ −5.2 eV). It is reasonable since the HOMOs are mainly localized onto the fluorenes and display π characters in PFTCNVT and PFTORT. Turning to the evolution of the LUMO levels, the LUMOs of PFTCNVT (∼ −2.7 eV) and PFTORT (∼ −2.8 eV) are generally stabilized by about 1.4 and 1.5 eV with respective to PF (∼ −1.3 eV) [46]. It is because the LUMOs are strongly confined to thienyl-based groups, the character of these thienyl-based moieties is decisive to the energy level of LUMOs. This indicates that the combination with electron-accepting moieties TCNVT and FTORT will both lower the LUMO energies and thus significantly improve the electron-accepting and transporting properties of the copolymers. The more planar conformations in both series under study relative to PF are also the reasons. Since HOMO shows inter-ring antibonding character and the LUMO shows inter-ring bonding character and the variation of torsional angles should have larger effects on LUMO. Indeed, the decreasing in the dihedral angles between the two adjacent subunits induced by the presence of the electron-accepting moieties TCNVT and FTORT should enhance the electron conjugation over the whole molecule and thus stabilize the LUMOs.

3.3. Ionic states properties

3.3.1. The optimized geometries in ionic states

As already mentioned before, one of the most important features of the π-conjugated polymers is their ability to become highly conducting after oxidative (p-type) or reductive (n-type) doping. So, the cationic and anionic geometries of oligomers in both series of $(FTCNVT)_n$ and $(FTORT)_n$ ($n=1$–4) are optimized by B3LYP/6-31G* and the inter-ring bond lengths and dihedral angles are compiled in Table 2. Compared the results in Tables 1 and 2, we found that the inter-ring distances $r(7,10)$, $r(13,15)$ and $r(18,20)$ decrease in the both cationic and anionic states in $(FTORT)_n$. The shortening of the inter-ring distances in ionic states relative to that in neutral state can easily be seen from the HOMO and LUMO characters plotted in Fig. 3. There is antibonding between the bridge atoms of inter-ring and there is bonding between the bridge carbon atom and its conjoint atoms of intra-ring in the HOMO. Hence, removing an electron from HOMO leads to a shortening of the inter-ring distances in cationic state relative to the neutral state. On the other hand, the LUMO of all the oligomers generally shows a bonding character between the two adjacent subunits. The shortening of the inter-ring distance in the anionic state is due to the bonding interactions between the π orbitals on the two adjacent fluorenes or thienyls. On the other hand, the injection of electrons or holes in these oligomers induces to the better conjugations than their corresponding neutral ground states. The dihedral angles between subunits of each oligomer in cationic and anionic states obviously decrease compared with their corresponding neutral states. In the cationic state of $(FTORT)_n$, the torsional angles of $\Phi(8,7,10,14)$, $\Phi(14,13,15,16)$ and $\Phi(19,18,20,21)$ are around 8.5, 17.9 and 22.2° which is even smaller than that in its anionic state. This indicates that the whole molecules tend to more planar with the injection of electrons or holes in these oligomers. In fact, the variation of bond lengths and dihedral angles for $(FTCNVT)_n$ follow the similar trends as shown in Table 2 with the same reasons.

3.3.2. Ionization potentials and electron affinities

The adequate and balanced transport of both injected electrons and holes are important in optimizing the performance of OLED devices. The ionization potential (IPs) and electron affinity (EAs) are well-defined properties that can be calculated by DFT on the geometries in the neutral, cationic and anionic sates to estimate the energy barrier for the injection of both holes and electrons into the polymer. Table 3 contains the ionization potentials (IPs) and electron affinities (EAs), both vertical (v; at the geometry of the neutral molecule) and adiabatic (a; optimized structure for both the neutral and charged molecule), and extraction potentials (HEP and EEP for

Table 3
Ionization potentials, electron affinities and extraction potentials for each molecule (in eV)

(eV)	IP (v)	IP (a)	HEP	EA (v)	EA (a)	EEP
(FTCNVT)$_n$						
$n=1$	6.52	6.38	6.25	0.12	1.33	1.44
$n=2$	5.97	5.86	5.76	1.83	1.93	2.01
$n=3$	5.75	5.67	5.60	2.08	2.16	2.22
$n=4$	5.63	5.56	5.50	2.22	2.29	2.35
$n=\infty$	5.34	5.28	5.25	2.60	2.64	2.69
Expl.	5.47			3.30		
(FTORT)$_n$						
$n=1$	6.53	6.34	6.17	1.47	1.68	1.85
$n=2$	6.03	5.89	5.76	2.04	2.18	2.30
$n=3$	5.83	5.73	5.64	2.28	2.37	2.46
$n=4$	5.72	5.65	5.57	2.40	2.47	2.55
$n=\infty$	5.42	5.42	5.40	2.75	2.76	2.80
Expl.	5.49			3.25		

The suffixes (v) and (a) indicate vertical and adiabatic values, respectively.

the hole and electron, respectively) that refer to the geometry of the ions [63–65]. The IP, EA, HEP, and EEP for infinite chains of the polymers were determined by plotting these values of oligomers against the reciprocal of the number of modeling polymeric units and by extrapolating the number of units to infinity.

One major problem with PFs for such applications is that they are usually much better at accepting and transporting holes than electrons. However, this drawback has been modified by the introduction of thienyl-based moieties. For PFTCNVT and PFTORT, the energy required to create a hole in the polymer is ∼5.3 and ∼5.4 eV, respectively, which is slightly smaller that in PF (5.5 eV) [46], suggesting the ability to create holes do not worsen by the introduction with electron-accepting thienyl-based moieties, which is consistent with the analysis for HOMO energy. On the other hand, the extraction of an electron from the anion requires ∼2.6 and ∼2.7 eV for PFTCNVT and PFTORT, which are largely higher than the corresponding PF (∼1.2 eV) [46] by around 1.4 and 1.5 eV, respectively. This indicates that the electron-accepting and transporting properties have been greatly improved in PFTCNVT and PFTORT compared with PF. Furthermore, the IPs and EAs obtained by three methods all agree well with the experimental data with the small errors in range of 0.07–0.22 eV for IPs and 0.45–0.70 eV for EAs. It is clear from these results that the introduction of electron-accepting moieties allows the modulation of the electron affinity. This should be useful to enhance the electron-transport from cathode in light-emitting diodes.

3.4. HOMO–LUMO gaps and the lowest excitation energies

Here, the HOMO–LUMO gaps (Δ_{H-L}s) and lowest singlet excited energies (E_g) are both listed in Table 4 and the relationships between the calculated Δ_{H-L} and the E_g and the inverse chain length are plotted in Fig. 5. There is a good linear relation between the energy gaps by both methods and the inverse chain length. In each case the energy gaps have the same trend to meet the experimental results. In fact, the theoretical quantity for direct comparison with experimental band gap should be the transition (or excitation) energy from the ground state to the first dipole-allowed excited state. The approach to get band gap with orbital energy difference between the HOMO and LUMO is crude considering experimental comparison. The implicit assumption underlying this approximation is that the lowest singlet excited state can be described by only one singly excited configuration in which an electron is promoted from HOMO to LUMO. In addition, the orbital energy difference between HOMO and LUMO is still an approximate estimate to the transition energy since the transition energy also contains significant contributions from some two-electron integrals. However, because the HOMO–LUMO gap is easy to get, the approach can also be used to provide valuable information on estimate band gaps of

Table 4
The HOMO–LUMO gaps (eV) and the lowest excitation energies (eV) of oligomers in (FTCNVT)$_n$ and (FTORT)$_n$

Oligomer	Δ_{H-L}	E_g (TD)	Oligomer	Δ_{H-L}	E_g (TD)
(FTCNVT)$_n$			*(FTORT)$_n$*		
$n=1$	2.97	2.91	$n=1$	2.90	2.66
$n=2$	2.58	2.40	$n=2$	2.59	2.34
$n=3$	2.46	2.24	$n=3$	2.50	2.26
$n=4$	2.41	2.20	$n=4$	2.46	2.21
$n=\infty$	2.22	1.93	$n=\infty$	2.30	2.08
Expl.	2.2[a]	2.2[b]	Expl.	2.2[a]	2.1[b]

[a] The data obtained from electrochemical measurements.
[b] Obtained from optical measurements in Ref. [45].

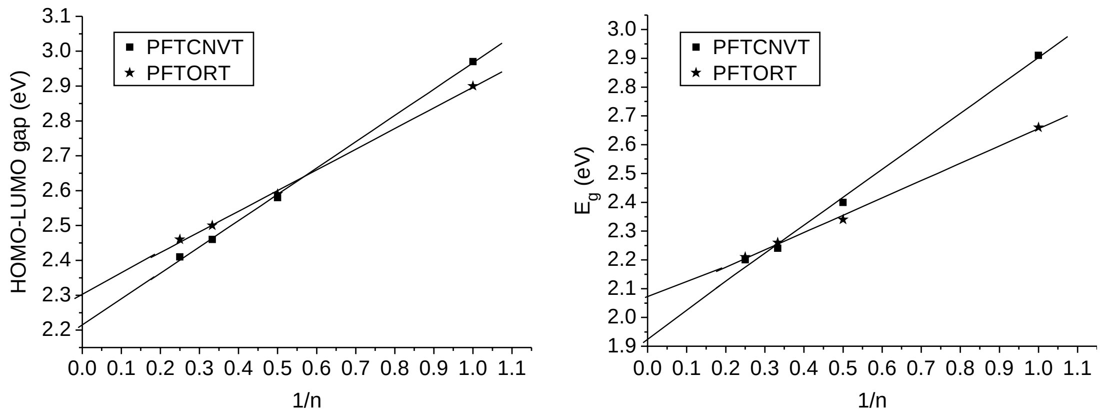

Fig. 5. The HOMO–LUMO gaps (right) the by B3LYP and lowest excitation energies E_g (left) by TD–DFT as a function of reciprocal chain length n in oligomers of $(FTCNVT)_n$ and $(FTORT)_n$.

oligomers and polymers, especially treating even larger systems [66,67].

Although for copolymers studied in this work, either HOMO–LUMO gap approach or TDDFT excitation energies provides reasonable good results, small errors still exist. Two factors may be responsible for deviations by both methods from experimental data. One is that the predicted band gaps are for the isolated gas-phase chains, while the experimental band gaps are measured in the liquid phase where the environmental influence may be involved. Another is that it should be borne in mind that solid-state effects (like polarization effects and intermolecular packing forces) have been neglected in the calculations. The latter can be expected to result in a decreased inter-ring twist and consequently a reduced gap in a thin film compared to an isolated molecule as considered in the calculations [68,69].

The band gaps obtained by TD–DFT and HOMO–LUMO gaps are 1.90 and 2.12 eV in PFTCNVT and 1.90 and 2.12 eV in PFTCNVT, respectively, which are even lower than the narrow band gap of PT (2.2 eV obtained experimentally) [70] and largely lower than that for PF (3.01 and 3.42 eV obtained by TD–DFT and HOMO–LUMO gaps [46]) by more than 1 eV, suggesting electron-accepting moieties TCNVT and TORT significantly decrease the energy gaps of fluorene-based copolymers. So we can estimate that the narrower band gaps of both PFTCNVT and PFTORT would lead to the long wavelength absorption and emission. It can be also concluded that the breaking of the conjugation in the backbone will broadened the energy gap and on the contrary, the good π-conjugated conformation should narrow the energy gap.

3.5. Absorption spectra

The TDDFT//B3LYP/6-31G* has been used to obtain the nature and the energy of the most relevant excited states of both series of oligomers on their ground-state equilibrium geometry and the absorption wavelengths, oscillator strengths and excitation character listed in Tables 5 and 6, respectively, together with the experimental absorption maxima.

As shown, all electronic transitions are of the ππ* type and involve both subunits of the molecule. In other words, no localized electronic transitions are calculated among the first five singlet–singlet transitions. In each oligomer of both series, the lowest lying singlet excited state S_1 is exclusively strongly optically allowed and dominated by a configuration in which an electron is excited from the highest occupied molecular orbital (HOMO) to the lowest unoccupied molecular orbital (LUMO). The excitation energies of the next four states are calculated to have relatively small oscillator strengths. Furthermore, the oscillator strength coupling the lowest CT π–π* singlet excited state to the ground state increase strongly when going from an isolated molecule to a molecular group. The oscillator strength associated with the S_1 state increases by about one order of magnitude upon adding one repeated unit to the monomers of PFTCNVT and PFTORT. Obviously, the strongest absorption peaks are all assigned to ππ* electronic transition character arising exclusively from $S_0 \rightarrow S_1$ electronic transition mainly composed by HOMO→LUMO transition. We can find that with the conjugation lengths increasing, the absorption wavelengths increase progressively as in the case of the oscillator strengths of $S_0 \rightarrow S_1$ electronic transition. It is reasonable, since HOMO→LUMO transition is predominant in $S_0 \rightarrow S_1$ electronic transition and as analysis above that with the extending molecular size, the HOMO–LUMO gaps decrease. Furthermore, we have calculated the absorption spectra of monomer and dimer of $(FTCNVT)_n$ in chloroform by polarizable continuum model (PCM) as implemented within the Gaussian 03 software package. The results show that the differences in wavelengths between the solvent and the gas phase are no more than 5 nm, suggesting that the solvatochromic effect is inappreciable in these systems under study. And this fitly reflects the fact observed in experiment that the discrepancies of UV–vis absorption between measured in solvent and measured in film are within 10 nm for both series.

From Tables 5 and 6 we find that our values by calculations of TDDFT overestimate the absorption spectra considering experimental data. Many investigations show that TDDFT is a good predictive tool for absorption spectra of molecules. However, this method has defects to study extended systems.

Table 5
Electronic transition data obtained by the TDDFT//B3LYP/6-31G* for $(FTCNV)_n$

Electronic transitions	Wavelengths (nm)	f	MO/character	Coefficient
FTCNVT				
$S_1 \leftarrow S_0$	426.51	1.0305	HOMO→LUMO	0.61
$S_2 \leftarrow S_0$	349.85	0.3129	HOMO-1→LUMO	0.52
			HOMO→LUMO+1	0.44
$S_3 \leftarrow S_0$	310.78	0.1221	HOMO→LUMO+1	0.42
			HOMO-1→LUMO	0.33
$S_4 \leftarrow S_0$	304.18	0.0006	HOMO-3→LUMO	0.45
			HOMO-2→LUMO	0.44
$S_5 \leftarrow S_0$	298.05	0.0035	HOMO-2→LUMO	0.51
			HOMO-3→LUMO	0.36
$(FTCNVT)_2$				
$S_1 \leftarrow S_0$	517.50	2.4933	HOMO→LUMO	0.65
$S_2 \leftarrow S_0$	466.81	0.1320	HOMO→LUMO+1	0.59
			HOMO-1→LUMO	−0.38
$S_3 \leftarrow S_0$	439.07	0.1133	HOMO-1→LUMO	0.53
			HOMO→LUMO+1	0.31
$S_4 \leftarrow S_0$	408.77	0.5328	HOMO-1→LUMO+1	0.61
$S_5 \leftarrow S_0$	385.24	0.0546	HOMO-3→LUMO	0.54
			HOMO→LUMO+2	0.31
$(FTCNVT)_3$				
$S_1 \leftarrow S_0$	553.81	3.1230	HOMO→LUMO	0.65
$S_2 \leftarrow S_0$	506.72	0.2250	HOMO-1→LUMO	0.51
			HOMO→LUMO+1	0.45
$S_3 \leftarrow S_0$	490.34	0.3822	HOMO→LUMO+1	0.47
			HOMO-1→LUMO	0.40
$S_4 \leftarrow S_0$	475.37	0.1017	HOMO→LUMO+2	0.56
			HOMO-2→LUMO	0.34
$S_5 \leftarrow S_0$	464.60	0.6363	HOMO-1→LUMO+1	0.59
			HOMO-2→LUMO	0.31
$(FTCNVT)_4$				
$S_1 \leftarrow S_0$	562.74	3.8828	HOMO→LUMO	0.62
$S_2 \leftarrow S_0$	518.36	0.7235	HOMO-1→LUMO	0.64
$S_3 \leftarrow S_0$	515.21	0.4988	HOMO→LUMO+1	0.65
$S_4 \leftarrow S_0$	492.41	0.2243	HOMO-1→LUMO+1	0.45
			HOMO→LUMO+2	0.44
$S_5 \leftarrow S_0$	491.30	0.3639	HOMO-1→LUMO+1	0.45
			HOMO-2→LUMO	0.42
Exp.	500[a]	500[b]		

[a] The data measured in solution.
[b] Measured in thin film in Ref. [45].

It is pointed out that TDDFT systematically overestimated the absorption spectra comparing to the experimental results due to the limitation of the current approximate exchange-correlation functionals in correctly describing the exchange-correlation potential in the asymptotic region [52,71]. However, reasonable results can still be expected here, because (1) we use the HF/DFT hybrid functional B3LYP, which could partially overcome the asymptotic problem [44,72,73] and because (2) we study the homologous fluorene-based cooligomers and polymers, with our interests in their modulation of electronic and optical properties by regular insertion of electron-accepting groups onto the pristine polyfluorene. The results show that both PFTCNVT and PFTORT have longer maximal absorption wavelength than PF(391 nm by TDDFT) [46]. This bathochrome to long wavelengths of the absorption maxima is ascribed to cooperation with the two thienyl-based accepting units and accords with the experimental observation and the estimation from energy gap.

3.6. Properties of excited structures and emission spectra

Density functional methods are, however, incapable of geometry optimization in designated excited states because of a lack of efficient algorithms for analytical gradients. Up to now, the standard for calculating excited state equilibrium properties of larger molecules is the configuration interaction singles (CIS) method. However, due to the neglect of electron correlation, CIS results are not accurate enough in many applications. In this study, we hope to investigate the excited state properties by this method, in despite of not accurate. Because the calculation of excited-state properties typically requires significantly more computational effort than is needed for the ground states and dramatically constrains by the size of the molecules, we only optimize the monomers of both series under study by CIS/3-21G*. In Fig. 6, we take the monomer of FTCNVT as an example to compare the excited state structure (S_1) by CIS/3-21G* with their ground state structure (S_0) by

Table 6
Electronic transition data obtained by the TDDFT//B3LYP/6-31G* for $(FTORT)_n$

Electronic transitions	Wavelengths (nm)	f	MO/character	Coefficient
FTORT				
$S_1 \leftarrow S_0$	465.57	0.9804	HOMO → LUMO	0.63
$S_2 \leftarrow S_0$	377.07	0.0738	HOMO-1 → LUMO	0.62
$S_3 \leftarrow S_0$	332.90	0.2330	HOMO → LUMO+1	0.56
			HOMO-1 → LUMO	0.19
$S_4 \leftarrow S_0$	314.06	0.0734	HOMO-2 → LUMO	0.53
			HOMO → LUMO+2	0.32
$S_5 \leftarrow S_0$	307.63	0.0034	HOMO-3 → LUMO	0.49
			HOMO-4 → LUMO	0.40
$(FTORT)_2$				
$S_1 \leftarrow S_0$	529.75	2.1945	HOMO → LUMO	0.65
$S_2 \leftarrow S_0$	481.21	0.1141	HOMO → LUMO+1	0.67
$S_3 \leftarrow S_0$	458.46	0.2330	HOMO-1 → LUMO	0.65
$S_4 \leftarrow S_0$	435.90	0.3555	HOMO-1 → LUMO+1	0.66
$S_5 \leftarrow S_0$	407.24	0.0254	HOMO-2 → LUMO	0.62
$(FTORT)_3$				
$S_1 \leftarrow S_0$	548.97	3.2509	HOMO → LUMO	0.64
$S_2 \leftarrow S_0$	499.62	0.2888	HOMO → LUMO+1	0.66
$S_3 \leftarrow S_0$	495.28	0.2342	HOMO-1 → LUMO	0.66
$S_4 \leftarrow S_0$	479.20	0.0185	HOMO → LUMO+2	0.65
$S_5 \leftarrow S_0$	467.51	0.5441	HOMO-1 → LUMO+1	0.64
$(FTORT)_4$				
$S_1 \leftarrow S_0$	560.15	3.9063	HOMO → LUMO	0.61
$S_2 \leftarrow S_0$	521.59	1.0671	HOMO → LUMO+1	0.46
			HOMO-1 → LUMO	0.45
$S_3 \leftarrow S_0$	510.30	0.1429	HOMO-1 → LUMO	0.46
			HOMO → LUMO+1	0.44
$S_4 \leftarrow S_0$	495.08	0.0383	HOMO → LUMO+2	0.56
			HOMO-2 → LUMO	0.29
$S_5 \leftarrow S_0$	490.85	0.4541	HOMO-1 → LUMO+1	0.62
Exp.	509[a]	510[b]		

[a] The data measured in solution.
[b] Measured in thin film in Ref. [45].

HF/3-21G*. Interestingly, the main characters of the front orbitals by HF/3-21G* are same to that by B3LYP/6-31G*. As shown, some of the bond lengths lengthened, but some shortened. We can predict the differences of the bond lengths between the ground (S_0) and singlet excited state (S_1) from MO nodal patterns. Due to the singlet state corresponds to an excitation from the HOMO to the LUMO in both considered oligomers, we can explore the bond lengths variation by analyzing the HOMO and LUMO. We know that the HOMO has a node across the $r(4',8)$, $r(9,10)$, $r(13',11')$ and $r(11,13)$ bonds in TCNVT, while the LUMO is bonding. The data confirm the anticipated contraction of these bonds. On the contrary, the HOMO is bonding across $r(4,5)$, $r(6,7)$, $r(2,7)$, $r(7',6')$, $r(2',7')$, $r(4',5')$, $r(3',4')$, $r(8,9)$, $r(10,11)$ $r(13,13')$, $r(11',10')$ and $r(8',9')$ in TCNVT, but the LUMO has nodes in these regions. Therefore, one would expect elongation of these

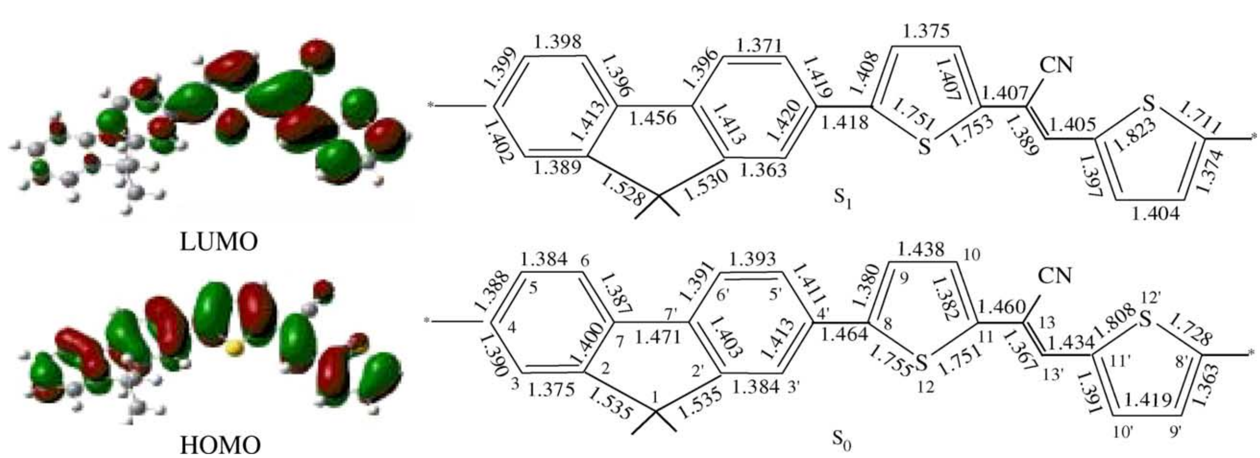

Fig. 6. Comparison of the excited structure (S_1) by CIS/3-21G* with the ground state geometry (S_0) by HF/3-21G* of the monomer of $(FTCNVT)_n$.

bonds; the data in the figure shows that these bonds are in fact considerably longer in the excited state.

The bridge bonds between each conjugation segment rotate to some extent when excited from ground to excited states. The biggest dihedral angle $\Phi(5',4',8,9)$ and in FTCNVT reduced from 37° by HF/3-21G* to nearly 0° from CIS/3-21G*. Similar with FTCNVT, the $\Phi(8',7',14,13)$, $\Phi(10,11,13,15)$ and $\Phi(15,13',11',10')$ in FTORT decrease from 38, 34 and 35° obtained by HF/3-21G* to 3, 14 and 19° by CIS/3-21G*, respectively. It is obvious that the excited structure has a strong coplanar tendency in both the series, that is, the conjugation is better in the excited structure, which further approves the predictions from frontier orbitals.

Consequently, the emission calculations are made by reoptimizations of the monomers FTCNVT and FTORT with the CIS/3-21G* method in their first singlet excited states, followed by using the resulting geometries to perform TD calculations employing the B3LYP/3-21G* method from the singlet ground state to the five singlet excited states. For FTCNVT the calculated fluorescence (473 nm) with strongest intensity (1.3795) for S_1 arising from HOMO→LUMO $\pi\pi^*$ excitation is close to the experimental result of 500 nm. The luminescence peak at 510 nm in PFTORT occurs in the same region of a singlet state S_1 calculated at 577.59 nm with largest oscillator strength, which corresponds to $\pi\pi^*$ excitation. In general, as the case of the absorption spectra, the emission wavelengths in FTCNVT and FTORT exhibits bathochromic compared with PF (434 nm by TDDFT) [46]. This is due to the more planar conformation with the presence of the electron-accepting moieties of TCNVT and TORT.

4. Conclusion

The oligomers of PFTCNVT and PFTORT show more planar structures compared with pristine polyfluorene (~37°) and polythiophene (~32°) [73]. All decisive molecular orbitals are delocalized on both subunits of the oligomers. The HOMO possesses an antibonding character between subunits, which may explain the non-planarity observed for these oligomers in their ground state. On the other hand, the LUMO shows bonding character between the two adjacent rings, in agreement with the more planar S_1 excited state. Importantly, the incorporation of fluorene and thienyl-based groups not only increase the PL quantum efficiency compared with those of conventional polythiophene materials, which is essential for light-emitting polymers, and provide the opportunity of tuning the electronic and optical properties of the resulting polymers but also maintain the low-band gap properties of polythiophene compared with polyfluorene and give rise to some interesting material.

Another advantage of the two series of oligomers and polymers under study is that the electron-accepting properties have been greatly improved than PF due to the electron-accepting thienyl-based groups and of course, the more planar conformation is also the reason. Excitation to the S_1 state corresponds almost exclusively to the promotion of an electron from the HOMO to the LUMO. Accordingly, the energy of the $S_0 \rightarrow S_1$ electronic transition follows the HOMO–LUMO energy gap of each oligomer. The first electronic transition gives rise to the largest values of the oscillator strength in each oligomer. The absorption and emission spectra of $(\mathrm{FTCNVT})_n$ and $(\mathrm{FTORT})_n$ exhibit red-shifted with the adding of thienyl-based groups compared with PF ascribed to the better conjugation backbones and the two series both emit a red–orange light.

Finally, this theoretical study confirmed experimental results where it was shown that the incorporated copolymers could greatly modulate and improve the electronic and optical properties of pristine polymers. Furthermore, using theoretical methodologies, we showed that is possible to predict reasonably the electronic properties of conjugated systems and we are convinced that the systematic use of those theoretical tools should contribute to orientate the synthesis efforts and help understand the structure–properties relation of these conjugated materials.

Acknowledgements

This work is supported by the Major State Basis Research Development Program (No. 2002CB 613406) and the National Nature Science Foundation of China (No. 90101026) and the Key Laboratory for Supramolecular Structure and Material of Jillin University.

References

[1] (a) Burroughes JH, Bradley DDC, Brown AR, Marks RN, Mackay K, Friend RH, et al. Nature 1990;347:539.
(b) Gustafsson G, Cao Y, Treacy GM, Klavetter F, Colaneri N, Heeger AJ. Nature 1992;357:477.
[2] (a) Yu G, Gao J, Hummelen JC, Wudl F, Heeger AJ. Science 1995;270:1789.
(b) Halls JJM, Walsh CA, Marseglia EA, Frienf RH, Moratti SC, Holmes AB. Nature 1995;376:498.
[3] Burroughes JH, Jones CA, Friend RH. Nature 1988;335:137.
[4] Yang Y, Heeger AJ. Nature 1994;372:344.
[5] (a) Pei Q, Yu G, Zhang C, Yang Y, Heeger AJ. Science 1995;269:1086.
(b) Pei Q, Yu G, Zhang C, Heeger AJ. J Am Chem Soc 1996;118:3922.
[6] Hide H, Dý'az-Garcý'a MA, Schwartz BJ, Andersson MR, Pei Q, Heeger AJ. Science 1996;273:1833.
[7] Kraft A, Grimsdale AC, Holmes AB. Angew Chem Int Ed 1997;37:4402.
[8] Friend RH, Gymer RW, Holmes AB, Buuroughes JH, Marks RN, Taliani C, et al. Nature 1999;397:121.
[9] Heeger AJ. Solid State Commun 1998;107:673.
[10] Tourillon G. In: Skotheim TJ, editor. Handbook of conducting polymers, vol. 1. New York: Marcel Dekker; 1986. p. 293.
[11] (a) Roncali J. Chem Rev 1992;92:711.
(b) Roncali J. Chem Rev 1997;97:173.
[12] McCullough RD. Adv Mater 1998;10:93.
[13] Berggren M, Inganäs O, Gustafsson G, Rasmusson J, Andersson MR, Hjertberg T, et al. Nature 1994;372:444.
[14] Andersson MR, Berggren M, Inganäs O, Gustafsson G, Gustafsson-Carlberg JC, Selse D, et al. Macromolecules 1995;28:7525.
[15] Inganäs O, Granlund T, Theander M, Berggren M, Andersson MR, Ruseckas A, et al. Opt Mater 1998;9:104.
[16] Beljonne D, Cornil J, Friend RH, Janssen RAJ, Bredas JL. J Am Chem Soc 1996;118:6453.
[17] Andersson M, Yu G, Heeger AJ. Synth Met 1997;85:1275.
[18] Yang Y, Pei Q, Heeger AJ. J Appl Phys 1996;79:934.

[19] Liu B, Yu W, Lai Y, Huang W. Chem Commun 2000;551.
[20] Sainova D, Miteva T, Nothofer H, Scherf U, Glowacki I, Ulanski J, et al. Appl Phys Lett 2000;76:1810.
[21] Weinfurtner K, Fujikawa H, Tokito S, Taga Y. Appl Phys Lett 2000;76:2502.
[22] Virgili T, Lidzey DG, Bradley DDC. Adv Mater 2000;12:58.
[23] Bernius M, Inbasekaran M, O'Brien J, Wu W. Adv Mater 2000;12:1737.
[24] Yu W, Pei J, Cao Y, Huang W, Heeger A. J Chem Commun 2000;76:2502.
[25] Oyaizu K, Iwasaki T, Tsukahara Y, Tsuchida E. Macromolecules 2004;37:1257.
[26] Peng Q, Lu ZY, Huang Y, Xie MG, Han SH, Peng JB, et al. Macromolecules 2004;37:260.
[27] Yang RQ, Tian RY, Yang W, Cao Y. Macromolecules 2003;36:7453.
[28] Yang NC, Lee SM, Yoo YM, Kim JK, Suh DH. J Polym Sci, Part A 2004;42:1058.
[29] Horst W, Susanne S, Stefan J, Alexander VU, Axel HEM. Macromolecules 2003;36:3374–9.
[30] Mushrush M, Facchetti A, Lefenfeld M, Katz HE, Marks TJ. J Am Chem Soc 2003;125:9414–23.
[31] Brédas JL, Silbey R, Boudreaux DS, Chance RR. J Am Chem Soc 1983;105:6555–9.
[32] Tavan P, Schulten K. J Chem Phys 1986;85:6602–9.
[33] Beljonne D, Shuai Z, Cornil J, dos Santos DA, Bredas JL. J Chem Phys 1999;32:267–76.
[34] Lahti PM, Obrzut J, Karasz FE. Macromolecules 1987;20:2023–6.
[35] Burrows HD, Seixas de Melo J, Serpa C, Arnaut LG, da Miguel NG, Monkman AP, et al. J Chem Phys 2002;285:3–11.
[36] Scheinert S, Schliefke W. Synth Met 2003;139:501–9.
[37] Yamamoto T, Fujiwara Y, Fukumoto H, Nakamura Y, Koshihara SY, Ishikawa T. Polymer 2003;44:4487–90.
[38] Morisaki Y, Ishida T, Chujo Y. Polym J 2003;35:501–6.
[39] Yang NC, Chang S, Suh DH. Polymer 2003;44:2143–8.
[40] Tavan P, Schulten K. J Chem Phys 1986;85:6602.
[41] Beljonne D, Shuai Z, Cornil J, dos Santos DA, Brédas JL. J Chem Phys 1999;111:6602.
[42] Kwon O, McKee ML. J Phys Chem A 2000;104:7106.
[43] Yu J-SK, Chen WC, Yu CH. J Phys Chem A 2003;107:4268.
[44] Ma J, Li SH, Jiang Y-S. Macromolecules 2002;35:1109–15.
[45] Beaupré S, Leclerc M. Adv Funct Mater 2002;12:192.
[46] Wang JF, Feng JK, Ren AM, Liu XD, Ma YG, Lu P, et al. Macromolecules 2004;37:3451.
[47] Lahti PM, Obrzut J, Karasz FE. Macromolecules 1987;20:2023–6.
[48] Winokur MJ, Slinker J, Huber DL. Phys Rev B 2003;67:184106.
[49] Donat-bouillud A, Lévesque L, Tao Y, D'Iorio M, Beaupré S, Blondin P, et al. Chem Mater 2000;12:1931–6.
[50] Zeng G, Yu WL, Chua SJ, Huang W. Macromolecules 2002;35:6907–14.
[51] Lee SH, Nakamura T, Tsutsui T. Org Lett 2001;3:2005–7.
[52] Wong KT, Wang CF, Chou CH, Su YO, Lee GH, Peng SM. Org Lett 2002;4:4439–42.
[53] Klaerner G, Miller RD. Macromolecules 1998;31:2007–9.
[54] Frisch MJ, Trucks GW, Schlegel HB, Scuseria GE, Robb MA, Cheeseman JR, et al. Gaussian 03, revision B.04. Pittsburgh PA: Gaussian Inc.; 2003.
[55] Foresman JB, Head-Gordon M, Pople JA. J Phys Chem 1992;96:135.
[56] Belletête M, Beaypré S, Bouchard J, Blondin P, Leclerc M, Durocher G. J Phys Chem B 2000;104:9118.
[57] Hay PJ. J Phys Chem A 2002;106:1634–41.
[58] Curioni A, Andreoni W, Treusch R, Himpsel FJ, Haskal E, Seidler P, et al. Appl Phys Lett 1998;72:1575–7.
[59] Sung YH, Dong YK, Chung YK, Roald H. Macromolecules 2001;34:6474–81.
[60] (a) Yang L, Ren AM, Feng JK, Liu XD, Ma YG, Zhang HX. Inorg Chem 2004;43:5961.
(b) Yang L, Ren AM, Feng JK, Ma YG, Zhang M, Liu XD, et al. J Phys Chem 2004;108:6797.
(c) Yang L, Ren AM, Feng JK. J Comput Chem 2005;26:969.
[61] (a) Ford WK, Duke CB, Salaneck WR. J Chem Phys 1982;77:5030.
(b) Ford WK, Duke CB, Paton A. J Chem Phys 1982;77:4564.
[62] Cornil J, Gueli I, Dkhissi A, Sancho-Garcia JC, Hennebicq E, Calbert JP, et al. J Chem Phys 2003;118:6615–23.
[63] Lin BC, Cheng CP, Michael Lao ZP. J Phys Chem A 2003;107:5241–51.
[64] Curioni A, Boero M, Andreoni W. Chem Phys Lett 1998;294:263–71.
[65] Wang I, Estelle BA, Olivier S, Alain I, Baldeck PL. J Opt Part A: Pure Appl Opt 2002;4:S258–S60.
[66] (a) Rogero C, Pascual JI, Gomez-Herrero J, Baro AM. J Chem Phys 2002;116:832–6.
(b) Curioni A, Andreoni W. IBM J Res Dev 2001;45:101–13.
[67] Wang JL, Wang GH, Zhao JJ. Phys Rev B 2001;64:205411.
[68] Puschning P, Ambrosch-Draxl C, Heimel G, Zojer E, Resel R, Leising G, et al. Synth Met 2001;116:327.
[69] Eaton VJ, Steele D. J Chem Soc, Faraday Trans 1973;2:1601.
[70] Roncali J. Chem Rev 1997;97:173–205.
[71] Tozer DJ, Handy NC. J Chem Phys 1998;109:10180.
[72] Gao Y, Liu C, Jiang Y. J Phys Chem A 2002;106:5380.
[73] Hsu C, Hirata S, Martin H. J Phys Chem A 2001;105:451.